Non-linear excitations in Ising-type magnetic chain systems I: Mossbauer relaxation studies of antiferromagnets in zero and applied field

Smit, H.H.A.; Groot, H.J.M. de; Elmassalami, M.; Thiel, R.C.; Jongh, L.J. de

Physica B 154 (1989) 237–253
North-Holland, Amsterdam

NON-LINEAR EXCITATIONS IN ISING-TYPE MAGNETIC CHAIN SYSTEMS I

MÖSSBAUER RELAXATION STUDIES OF ANTIFERROMAGNETS IN ZERO AND APPLIED FIELD*

H.H.A. SMIT, H.J.M. DE GROOT, M. ELMASSALAMI,** R.C. THIEL and L.J. DE JONGH
Kamerlingh Onnes Laboratorium, Rijksuniversiteit Leiden, Postbus 9506, 2300 RA Leiden, the Netherlands

Received 3 October 1988

Temperature and field dependent Mössbauer effect spectroscopy measurements on the Ising-type antiferromagnetic chain systems $FeC_2O_4 \cdot 2H_2O$ and $RbFeCl_3 \cdot 2H_2O$ are reported. The spectra of these systems show relaxation behaviour over a large temperature range which can be explained in terms of non-linear excitations. The influence of an applied magnetic field has been studied. An attempt to describe the excitations by the ideal kink gas resulted in three major discrepancies. We discuss a phenomenological model which is based on the excitation spectrum of the Ising-type chain system and which is compatible with the present data and the experimental data in the current literature.

1. Introduction

In recent years one-dimensional (1D) magnetism has gained renewed interest, since it has proven to generate model systems for investigating non-linear excitations, see e.g. ref. [1]. Non-linear excitations, as solitons or kinks, are local excitations that connect degenerate ground states. In a ferromagnet, a π-soliton separates a spin up and spin down region (fig. 1a). Similar π-solitons separate degenerate ground state configurations of the antiferromagnetic chain, which are obtained by a simultaneous rotation of the spins of the two sublattices over an angle π (fig. 1b). We will use the term soliton for the large amplitude solutions of a non-linear differential equation (e.g. the sine–Gordon equation). In highly anisotropic systems, the soliton width decreases to zero, as depicted for an antiferromagnetic system in fig. 1c. We will refer to these "narrow" solitons as kinks. Under the assumption that the solitons (kinks) neither interact with other solitons (kinks) nor with the lattice, they can be described in the ideal gas approximation. These free solitons (kinks) have the intriguing characteristic that their energy is preserved when they are translated along the chain, which means that an initially given momentum is constant during the propagation. The dynamic behaviour of the solitons (kinks) determines the spin correlation function. With the Mössbauer effect, one probes the autocorrelation function, $\langle S^z(0) S^z(t)\rangle$, of the electronic spins on the magnetic chains. Mössbauer effect spectroscopy (MES) has proven to be a very valuable tool for observing the dynamics of kinks, since its frequency window (10^5 to 10^9 Hz) is well below that of neutron diffraction measurements. It carries, therefore, information about the long-time correlations of the electronic spins inaccessible to the neutron scattering technique.

In earlier papers and theses of our group, it has been shown that relaxation behaviour, resulting from non-linear excitations, appears both in ferro- and antiferromagnetic Ising-type chain systems at temperatures roughly between T_c and $3T_c$, where T_c is the three-dimensional (3D) ordering temperature [2–7]. In this temperature regime the compounds are 1D model systems, since the intra-chain interactions are larger than the thermal energy, $k_B T$, resulting in strong 1D correlations, whereas the inter-chain interactions

* This paper is the first of a series of three, all published in this issue.

** Present address: Physics Department, University of Khartoum, P.O. Box 321, Khartoum, Sudan.

that cause the 3D ordering at T_c, are still too weak to play an important role. In the earlier work, the measured spectra seemed to fit the stochastic model for the MES line shape of Blume and Tjon quite well, which made it possible to evaluate relaxation frequencies in MHz. The activation energy, as determined from the electronic flip rate as a function of the inverse temperature, was systematically found to be twice the energy of a single kink, that is, it corresponds to the energy of a kink pair (see fig. 1d). This posed a problem for some time, since ideal kink gas descriptions predict the activation energy to be that of a single kink. Moreover, MES experiments on $Fe(NH_5)_2(SO_4)_2$ showed the superposition of two subspectra in a compound with only one crystallographic iron site [8]. This could be interpreted in terms of a slowly and a fast relaxing subspectrum, of which the static Mössbauer parameters are identical [4]. The slowly relaxing subspectrum showed again the activation energy of twice the kink energy, whereas the fast relaxing subspectrum gave a temperature independent relaxation rate. AC susceptibility absorption (χ'') measurements between 10 and 10^5 Hz on the doped Ising-type ferromagnetic compounds $M_xFe_{1-x}Cl_2(Py)_2$ (where M is Ni, Cd, Mn, or Co, and Py is NC_5H_5) have revealed the activation energies of both single kinks and kink pairs [5, 6].

The first system we report upon in this paper, $FeC_2O_4 \cdot 2H_2O$, not only shows an activation energy of twice the soliton energy, but also shows systematic deviations between the MES data and the spectra generated by the stochastic model of Blume and Tjon. We have chosen this particular antiferromagnetic Ising-type chain system, since it has a very pronounced 1D character and its magnetic characteristics are well known in the literature. The intra-chain exchange interaction, J, and the 3D ordering temperature, T_N, have been reported in independent experimental investigations, namely specific heat and susceptibility studies. Moreover, the hyperfine field in the present system is typically 3 times as large as in the compounds reported earlier [3, 7]. The experimental resolution in the relaxation regime is therefore much larger, which allows one to better distinguish between the different propagation mechanisms for the kinks, and investigate the shortcomings of the ideal kink gas model. It is interesting to note that already the first NMR experiments on both planar TMMC ($(CH_3)_4NMnCl_3$) and Ising-type $RbFeCl_3 \cdot 2H_2O$ indicated deviations from the ideal kink gas behaviour [9, 10]. More recently, low energy neutron scattering and neutron spin echo experiments on TMMC also showed shortcomings of the ideal kink gas description [11, 12].

In order to investigate the influence of an applied magnetic field on the dynamics of non-linear excitations, MES experiments on single crystal absorbers have been performed. A suitable candidate is the Ising-type chain system

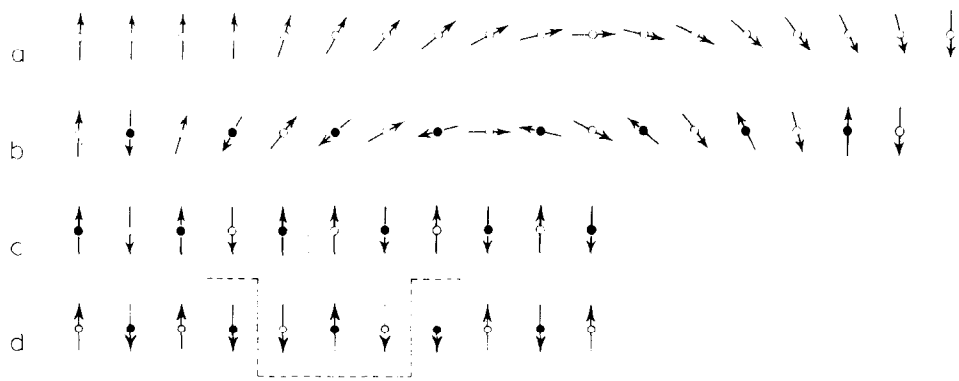

Fig. 1. Non-linear excitations in magnetic chains: (a, b) π-soliton in a classical ferro- and antiferromagnetic chain, and (c,d) single kink and a kink pair excitation in a quantum mechanical $S = 1/2$ antiferromagnetic chain (schematic).

$RbFeCl_3 \cdot 2H_2O$, since large single crystals can be grown*. Its magnetic quantities, T_N and J, have been determined by various magnetic specific heat, magnetization, and susceptibility studies. The electronic spins are ordered antiferromagnetically in a slightly canted configuration. The presence of the resulting ferromagnetic components provides the possibility of overcoming the inter-chain coupling and suppressing the 3D ordering temperature to zero by applying a moderate magnetic field parallel to these ferromagnetic components. In this way, the influence of the 3D ordering temperature can be studied.

This paper will be arranged as follows. In section 2 we will give the details of the magnetic properties of the investigated compounds. Section 3 will deal with the MES spectra and elucidate the method of analysis. The discrepancies between the ideal non-interacting kink gas and the experiment will be discussed in section 4. In section 5 we will propose a phenomenological model which explains the present data and is compatible with the AC susceptibility absorption (χ'') experiments, see refs. [5, 6] and the following paper. Subsequently, the MES results will be compared to NMR and neutron scattering experiments reported in the recent literature (section 6).

2. Properties of the investigated compounds

In this paper we shall study two quasi 1D Fe^{2+} magnetic systems by means of the ^{57}Fe Mössbauer effect. The chain systems under investigation are antiferromagnetically coupled in the chain, and have a large intra- to interchain interaction ratio.

The first compound, α-$FeC_2O_4 \cdot 2H_2O$ or Fe-oxolate, hereafter referred to as FOX, is known in the literature for quite some years. The structure, as determined by P.C. Carić [13], can be described by the monoclinic space group C2/c with unit cell dimensions $a = 12.04$ Å, $b = 5.58$ Å, $c = 9.89$ Å, and with $\beta = 127°34'$. It is found that the FeC_2O_4 units form a linear chain along the b direction (see fig. 2a, drawn after Carić). The delocalized π-electrons of the oxalate group serve as an effective intermediary for significant superexchange along the chain [14]. The chains are separated by the water molecules in one direction, whereas the exchange path in the third direction is also quite long (i.e. Fe–O2–O4'–Fe', see fig. 2b). The ferrous ion is surrounded by a distorted octahedron formed by a rectangle of oxygens of the oxalate groups and two oxygens belonging to the water molecules.

In earlier work, the Mössbauer data [15, 16] have been misinterpreted by attributing the line broadening, observed between about 10 and 25 K, to an additional strucuture or some cooperative effect. Also, from these data, the 3D ordering temperature was estimated incorrectly as $T_N = 26$ K. Only recently the 3D ordering temperature has unambiguously been determined from a small maximum in the specific heat

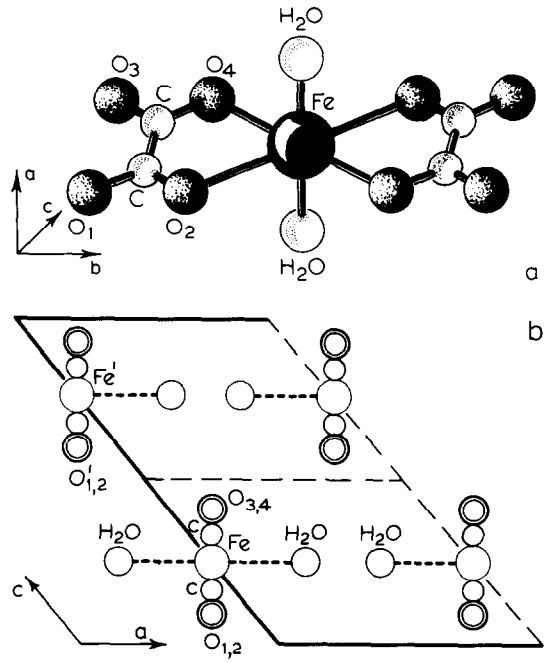

Fig. 2. (a) Schematic representation of the crystallographic structure of $FeC_2O_4 \cdot 2H_2O$, and (b) a projection on the ac plane of the atomic positions in the unit cell.

* We thank the group of Prof. Dr. W.J.M. de Jonge of the Technische Universiteit te Eindhoven, The Netherlands for providing the crystals.

at 11.7 K [17]. This was confirmed by subsequent neutron diffraction eperiments on $FeC_2O_4 \cdot 2D_2O$, reported upon in the same reference. FOX is a very good 1D system, as can be inferred from the size of the peak in the specific heat that accompanies the 3D ordering. Most of the magnetic entropy is removed by the 1D correlations, leaving only a small fraction for the 3D ordering. The crystal field levels have been determined from ligand field spectra and the temperature dependence of the quadrupole splitting [18]. The lowest spin quintuplet shows a nearly degenerate doublet as the ground state, the next excited state being at about 60 K. At temperatures low compared to this splitting, only the ground state doublet is populated, resulting in a description of the magnetic properties within the effective spin $S = \frac{1}{2}$ Hamiltonian,

$$\mathcal{H} = -2J \sum_i (S_i^z S_{i+1}^z + \varepsilon S_i^x S_{i+1}^x + \varepsilon S_i^y S_{i+1}^y) . \tag{1}$$

The large single-ion anisotropy is reflected in a strong anisotropy in the exchange constant, i.e. $\varepsilon \ll 1$. The magnetic susceptibility was fit by the first (Ising) term of this Hamiltonian, yielding $J/k_B = -82.6$ K [17].

We have also examined an Fe-oxalate compound with a substitution of the water molecules by Imidazole (Iz or $C_3N_2H_4$). The crystal field at the iron sites changes drastically by this substitution, since the nitrogen atoms enlarge the distortion of the octahedral surrounding. This results in a change of sign of the observed quadrupole splitting, and the spin anisotropy changes from Ising- to XY-type. From the temperature dependence of the hyperfine field we estimate the 3D ordering temperature as 5.4 K. Since the MES measurements do not show relaxation behaviour over a large temperature range in this compound, the estimation of the 3D temperature by the MES experiments can be trusted to within a few tenths of Kelvin. An attempt has been made to calculate the crystal field levels. This gave a lowest spin quintuplet, with a singlet as the ground state and the first excited doublet at a few Kelvin, resulting in a negligible easy axis anisotropy in the easy plane. The value of η, which is 0.6, as found in ref. [16] and confirmed by our experiment, probably finds its origin in a difference in direction of the main axes of the electric field gradient contributions due to the lattice and due to the valence electrons.

The second compound is $RbFeCl_3 \cdot 2H_2O$, which will be denoted as RFC in what follows. Large single crystals, with typical dimensions of $2 \times 2 \times 0.5$ cm^3, were grown by slow evaporation of anhydrous $FeCl_2$ and RbCl in a 0.03N solution of HCl. The nearly transparent crystals are stable in normal atmosphere and may be cleaved easily along the *ab* plane. The crystallographic structure as determined by neutron diffraction experiments [19] can be described by the orthorhombic space group P2/c2/c2/a. The unit cell accommodates four formula units and has the dimensions $a = 8.876$ Å, $b = 6.872$ Å, and $c = 11.181$ Å at 4.2 K. The magnetic structure of RFC as reported in the literature [19] is shown in fig. 3a. The antiferromagnetic chains are along the *a* axis, where the chlorine ions give rise to the superexchange interaction between the ferrous ions. The magnetic interaction in the *b* direction is two orders of magnitude smaller than in the *a* direction, since the chains are separated by the Rb ions. The magnetic interactions along the *c* axis, where the water molecules separate the chains, are again weaker. Magnetic specific heat measurements revealed a sharp anomaly at 11.96 K, indicating the 3D ordering [20]. They could best be fit by the rectangular $S = \frac{1}{2}$ Ising model with an intra-chain interaction $J_a/k_B = -39$ K and an inter- to intra-chain interaction ratio $J_b/J_a = 2 \times 10^{-2}$. Single crystal susceptibility measurements [21] and the temperature dependency of the quadrupole splitting [8] could be

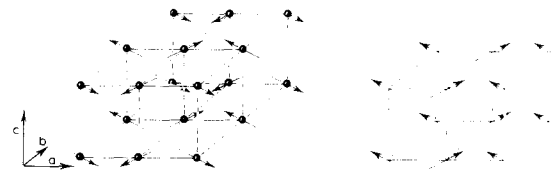

Fig. 3. Representation of the magnetic structure of $RbFeCl_3 \cdot 2H_2O$ (left) at zero field and temperature and (right) as proposed at $B_c > 1.24$ T and zero temperature.

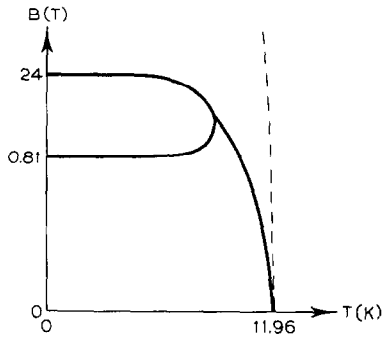

Fig. 4. A schematic representation of the phase diagram for $RbFeCl_3 \cdot 2H_2O$, drawn after ref. [21]. The solid and the broken lines represent the phase boundaries if the applied field is parallel to the ferro- and antiferromagnetically aligned spin components, respectively.

explained by a lowest spin quintuplet that shows a nearly degenerate doublet ground state, with the next excited state at 60 K. This indicates that the magnetic properties of RFC below this temperature can be described by an effective spin $S = \frac{1}{2}$ Hamiltonian (eq. 1).

In RFC, the magnetic moments are slightly canted by an angle of 19° from the *a* axis towards the *c* direction. This results in weak ferromagnetically ordered components in the *c* direction, which however alternate in going from one *ac* plane to the next (fig. 3a). For an applied field $B_c = 0.81$ T along the *c* axis, a first order spin transition occurs [21], and for $B_c > 1.24$ T, the weak ferromagnetic components are aligned parallel to the field in the magnetic structure shown in fig. 3b (at $T = 0$ K). In this way the 3D ordering temperature can be completely suppressed in a moderate applied field. A schematic representation of the phase diagram, drawn after ref. [21], can be found in fig. 4.

3. Experimental

The ^{57}Fe Mössbauer measurements were performed in a vertical cryostat in which both the source and the absorber were cooled. A standard drive system was operated in the constant acceleration mode. The multichannel spectrometer was microprocessor based. Velocity calibration was done in situ with a He–Ne laser and Michelson interferometer.

The temperature measurement of the absorber was carried out with a four point AC bridge, utilizing a glass–carbon resistance thermometer calibrated in our laboratory [22]. In a magnetic field the resistance value has been corrected as proposed by Sample [23]. The measurement stability, reproducibility, and accuracy were in all cases better than 0.5%. A superconducting solenoid with a maximum field of 7.5 T and provided with a cancellation coil to prevent the source being split by the applied field was used in persistent mode. Great care was taken for the orientation of the single crystals. After rubbing the crystals down to a thickness of 0.1 mm they were oriented to within 1 to 2 degrees using the Laue method of X-ray scattering.

3.1. Excess linewidth

Some representative powder spectra of FOX are shown below in fig. 7. First inspection of the spectra leads to the conclusion that the resonance lines are broadened over a large temperature range. It is obvious from these spectra that the hyperfine field does not decrease to zero at the three-dimensional ordering temperature, T_N, which was determined by an independent experimental technique (i.e. specific heat) as 11.7 K [17]. The effective hyperfine field is, therefore, not proportional to the spontaneous magnetization, so that T_N cannot be determined from MES experiments. The excess linewidth is caused by slow fluctuations of the hyperfine field. Other mechanisms, like a distribution of Néel temperatures as suggested and subsequently rejected by Le Fever [8], can also be ruled out here on basis of the pronounced sharp peak in the specific heat measurements. Another possibility would be a distribution of hyperfine fields. This is, however, very unlikely, since FOX is a completely regular crystalline solid, in which a regular 3D magnetic ordering of the moments below T_N is observed in neutron diffraction experiments [17].

As a first trial, we have analysed the measured spectra in terms of Lorentzians. (N.B. These fits

are not those shown in fig. 7.) At low temperatures, the fluctuations of the hyperfine field are slow compared to the nuclear level splitting (i.e. $\Gamma_\omega < \delta$, where 2δ is the energy difference of the two transitions that are coupled by the fluctuating hyperfine field). Eight Lorentzians are observed, which have been fitted with four symmetric doublets with equal splitting and intensity [24]. The excess linewidths were assumed to be equal for all lines [25]. In the high frequency region, $\Gamma_\omega > \delta$, the spectra show a doublet with Blume asymmetry. These spectra can be analysed using a doublet with two independent parameters for the linewidths. The averaged results for the linewidth are shown in fig. 5.

This figure shows that anomalous line broadening appears over a large temperature range, i.e. between $\sim T_N$ and $\sim 3T_N$. Critical fluctuations accompanying the 3D ordering cannot account for the observed anomaly, since they will only be present in the temperature range $t = |T - T_N|/T_N < 0.1$.

The anomalous line broadening has been observed in a large number of systems [2–7], all of which are characterized by a large Ising-type magnetic anisotropy. Counter examples are e.g. the $FeC_2O_4 \cdot (Iz)_2$ and $^{57}Co{:}Co(SO_4)_2(N_2H_5)_2$, which both show planar (XY-type) anisotropy. For the former, this is experimentally shown by the curve of the excess linewidth in fig. 5. Mössbauer source measurements on the latter also lack any slow relaxation behaviour [2]. The absence of slow relaxation behaviour can be understood from the fact that the elementary excitations in the XY systems are spin waves and not solitons [26] (the same argument holds for Heisenberg systems). The fluctuation frequencies are then of the order of 10^{12} Hz, which is much faster than the characteristic Mössbauer frequency. Consequently, the hyperfine field is proportional to the thermally averaged spin value (or sublattice magnetization) over the complete temperature range. For kink-type excitations to occur, a symmetry breaking Ising component, and thus a degeneracy of the ground state, is a necessary prerequisite.

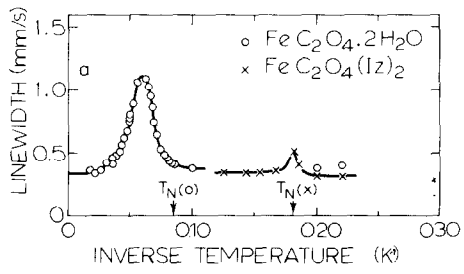

Fig. 5. Mössbauer linewidth versus inverse temperature for the two Fe-oxalate compounds.

As a comparison with our data, we want to mention the results on a dilute Fe compound, since it gives interesting information about the relaxation mechanism involved. The Mössbauer spectra of $Fe_xZn_{1-x}(SO_4)_2(N_2H_5)_2$, with $x = 0.07$, [8] show a single narrow doublet at temperatures down to 4.2 K, and any excess linewidth, as has been observed in the pure Fe compound ($x = 1$) up to much higher temperatures, is absent. As the majority of the ferrous ions (~85%) are surrounded by non-magnetic Zn ions, this observation excludes single-ion relaxation as a possible source for the anomalous line broadening in our quasi 1D anisotropic magnetic systems.

3.2. *Powder data and the Blume and Tjon model*

To obtain more information from the measured spectra we have employed the relaxation model of Blume and Tjon [27, 28]. In what follows, it will be referred to as the BT model. A square matrix of size 16, including the indices for the ground and excited nuclear states as well as the stochastic index $\sigma = \pm 1$, is diagonalized to find the transition energies and intensities. Especially if $\Gamma_\omega \approx \delta$, the BT model provides a way to study the spectra more reliably than the above described method using Lorentzians. Moreover, the BT model has the advantage that non-adiabatic effects can be taken into account [28]. And finally, since the BT model is based on a stochastic Markov process, this immediately checks whether the relaxation mechanism causes the electronic spins to flip randomly in time. No perpendicular hyperfine field components were considered, since the anisotropy constants are large compared to the temperature. Therefore

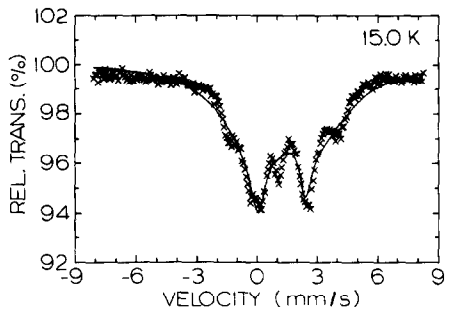

Fig. 6. Mössbauer spectrum of $FeC_2O_4 \cdot 2H_2O$ at 15 K. The solid line represents the best obtainable fit using the Blume and Tjon model with a single relaxation frequency.

the main components of the spins are along the easy axis. The same reasoning is used in ref. [29] to justify the neglect of the contribution of the fluctuations of the perpendicular hyperfine field components to the nuclear spin lattice relaxation.

As is shown in fig. 6, the BT model does not give an acceptable fit for FOX. In this respect, the magnitude of the hyperfine field is crucial, because it is only for the present large hyperfine field values ($H_{hf} = 15.0$ T) that the spectra have enough structure and detail in the relaxation regime for the deviations between the data and the fit to become apparent. It is very important to realize that, since the BT model does not fit the data, one may conclude that the effective hyperfine field does not fluctuate randomly in time with a single fluctuation rate for all Mössbauer sites.

An alternative is prompted by the deviations of the fitted line from the data in fig. 6, since the data still show several additional Mössbauer lines originating from a hyperfine split subspectrum. The spectra are assumed to consist of two subspectra with equal static MES parameters (IS, QS, Γ_0, and H_{hf}^0), but different relaxation rates. In several representative spectra (see fig. 7)

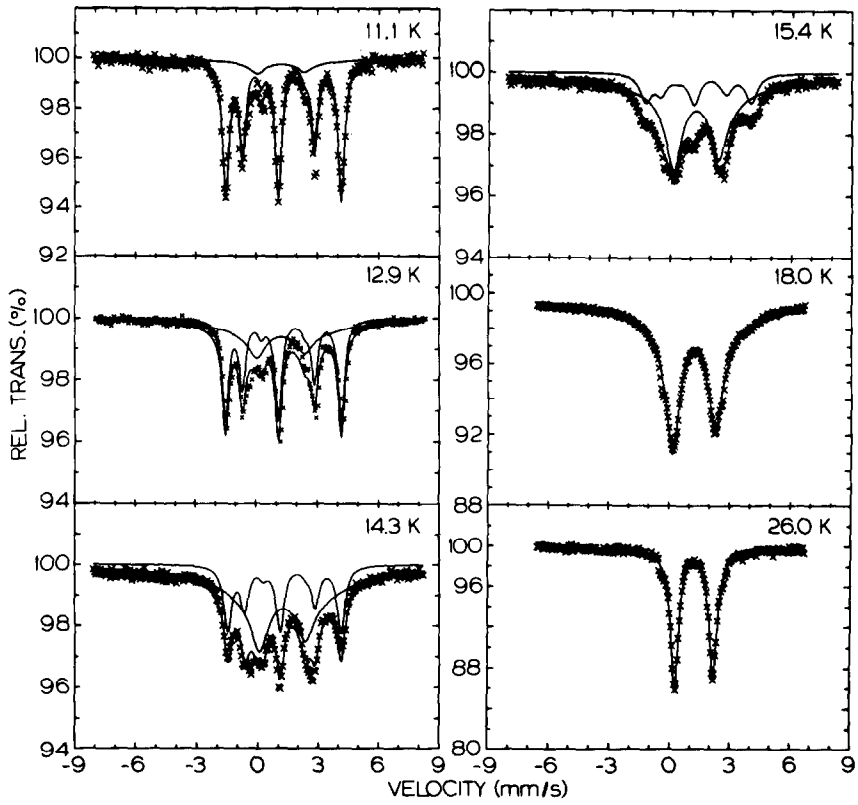

Fig. 7. Representative MES powder spectra of $FeC_2O_4 \cdot 2H_2O$ at various temperatures. The solid lines represent the two subspectra generated by the Blume and Tjon model and their superposition.

Table I
Static MES parameters determined at 4.2 K. The IS is relative to ^{57}Co:Rh at room temperature.

	FOX	$FOX(Iz)_2$	RFC
IS (mm/s)	1.21(0.02)	1.11(0.02)	1.19(0.02)
QS (mm/s)	−1.88(0.02)	2.06(0.02)	−1.36(0.02)
η	0.7(0.1)	0.6(0.1)	0.6(0.1)
H_{hf}^0 (T)	15.0(0.1)	5.3(0.1)	7.4(0.1)
θ (deg)	84(5)	72(5)	29(2)
ϕ (deg)	90(20)	90(20)	46(20)

these distinct contributions are separately shown. As can be seen in these figures, very acceptable fits are obtained. The compounds studied in our earlier papers did not exhibit such large hyperfine fields, and were initially fit by a single relaxation spectrum. However, a refit with the here described procedure also gave better results. In table I the static Mössbauer parameters are given, which are in agreement with earlier publications, both for FOX [15] and for RFC [8]*.

In figs. 8 and 9, the logarithm of the flip rates of both the relatively slowly and fast relaxing subspectra are plotted versus the inverse temperature for FOX and RFC respectively. The flip rate of the relatively slowly relaxing subspectrum can be described by a thermal activation process:

$$\Gamma_\omega \propto \exp(-E_a/k_B T) . \quad (2)$$

The activation energies, E_a, are 150(20) K and 110(10) K for FOX and RFC respectively. These activation energies correspond to roughly twice the intra-chain exchange energy, i.e. $2J/k_B$, since this amounts to 165 and 78 K, respectively. The relatively fast relaxing component shows a temperature independent relaxation rate of about 40 and 10 MHz for FOX and RFC, respectively. Above a certain temperature, the intensity of the slowly relaxing subspectrum becomes

* Some of the powder results of RFC were obtained from a refit of the data measured by H.Th. Le Fever.

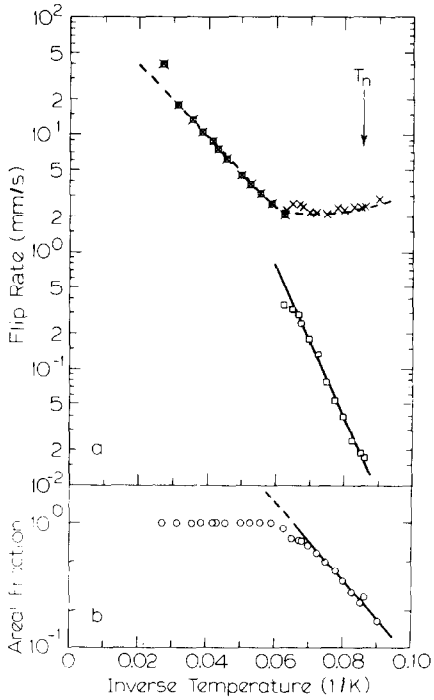

Fig. 8. The flip rate of the slowly (□) and fast (×) relaxing subspectra of $FeC_2O_4 \cdot 2H_2O$. The lower part shows the relative intensity of the fast relaxing component. The solid lines illustrate the activated processes.

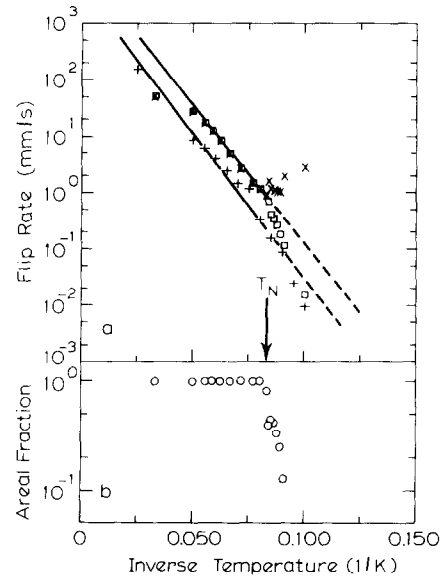

Fig. 9. The flip rate of the slowly (□) and fast (×) relaxing subspectra of the powder measurements on $RbFeCl_3 \cdot 2H_2O$. (+) represents the flip rate obtained from the measurements in a field of 3 T along the *a* axis. The lower part shows the relative intensity of the fast relaxing component for the zero field data.

negligible, such that only a single spectrum was sufficient to fit the experiment. In figs. 8 and 9, also the intensity of the doublet is plotted versus the inverse temperature for each compound. As is clearly seen, the intensity of the doublet increases monotonically as a function of the temperature. In the RFC compound, a jump in the relative area of the fast relaxing subspectrum occurs at the 3D ordering temperature.

3.3. *Single crystal results in an applied field*

First we will discuss the results of the application of a magnetic field of 3 T along the crystallographic *a* axis of RFC. Since the field is directed along the antiferromagnetically aligned components of the spins (fig. 3) and the exchange field is of the order of 15 T, the influence of the field on the 3D ordering temperature can be neglected (see fig. 4). Representative spectra are shown in fig. 10. At the lowest temperatures, the contributions of the two sublattices can be observed separately, since the effective hyperfine field is the vector sum of the applied field and of the internal field originating from the electrons. At the highest temperatures, the internal hyperfine field fluctuation frequencies are much higher than the Mössbauer frequency window, such that the internal hyperfine field is proportional to the thermally averaged spin value $\langle S_z \rangle$. The spectra were fitted by the BT model, assuming the applied field and the quadrupole splitting to be static, and the internal hyperfine field to jump randomly between $+H_{hf}$ and $-H_{hf}$. The probabilities for the spin being parallel and anti-parallel to the applied field were allowed to be unequal. The static hyperfine parameters were determined at 4.2 K and kept at these values at higher temperatures. Within the experimental accuracy, these parameters correspond to the powder values in table I. The applied field was fixed at 3 T. The polar and azimuthal angles of the γ-rays and the applied field relative to the main axis of the EFG were found to be 30(5)° and 45(20)°, i.e. parallel to the internal hyperfine field, in agreement with ref. [8]. From the fits, shown by the solid lines in fig. 10, it can be concluded that a single fluctuation rate for all Mössbauer sites is sufficient for fitting the spectra. This is in contrast to the powder measurements as discussed in section 3.2. The resulting fluctuation rates can be found in fig. 9. An activation energy of 119 (15) K is

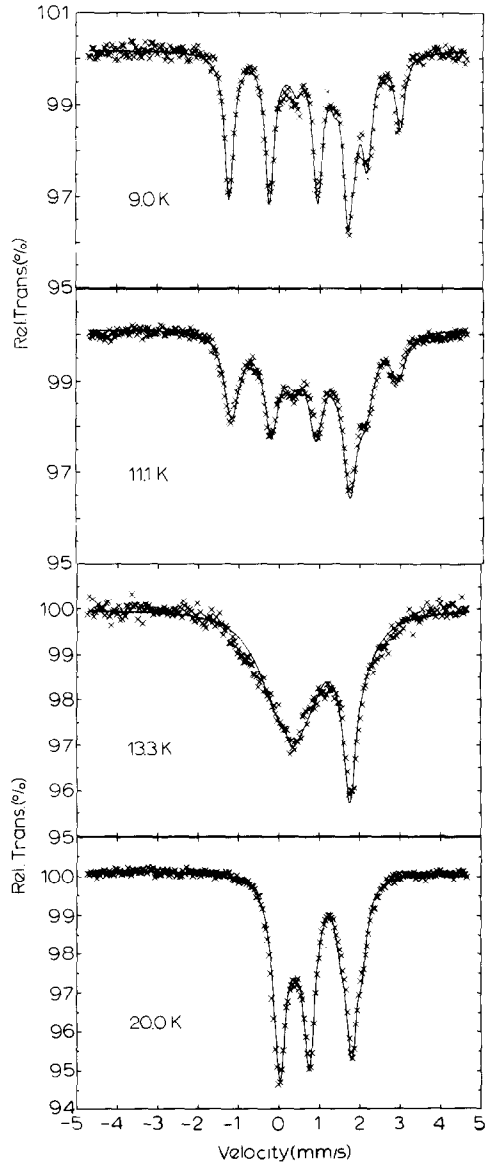

Fig. 10. Representative single crystal spectra of $RbFeCl_3 \cdot 2H_2O$ measured in a field of 3 T along the *a* axis. The solid lines represent the fit using the Blume and Tjon model.

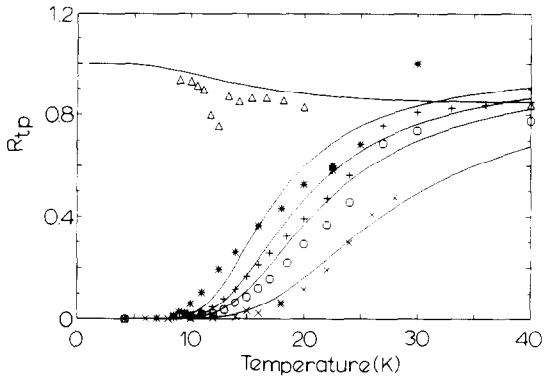

Fig. 11. Ratio of transition probabilities, R_{tp}, of $RbFeCl_3 \cdot 2H_2O$ versus temperature for $B_a = 3\,T$ (△) and $B_c = 1.5$, 2.25, 3.0, 6.0 T (*, +, ○, ×, respectively). The solid lines represent the predictions for an ideal $S = 1/2$ Ising chain.

obtained, which corresponds to the powder value. Below the 3D ordering temperature, the fluctuation rate falls off steeper than for an activated process. The ratio of transition probabilities, hereafter referred to as R_{tp}, is defined between 0 and 1. It is plotted in fig. 11, where it is shown to be comparable to the prediction for the Ising chain [30], with $J_a/k_B = -39\,K$, $B = (\mu_a/\mu_B)B_{app}$, where $B_{app} = 3\,T$ and $\mu_a = 4.6\mu_B$ [21]. Evidently this model neglects the 3D ordering, and one can see the strongest deviations at temperatures where 3D critical fluctuations are likely to be present.

Subsequently, magnetic fields of 1.5, 2.25, 3.0, and 6.0 T were applied along the c axis. Representative spectra are shown in fig. 12. These fields are sufficiently strong to align the ferromagnetic components of the spins parallel to the field at $T = 0\,K$. As a result, at the lowest temperatures only one magnetic site remains, and the spectra show one octet. The corresponding R_{tp} is equal to zero. At the highest temperatures, the observed octet has a hyperfine field that is the vector sum of the applied field and the internal field, which is proportional to $\langle S_z \rangle$. The spectra were analysed using the BT model, with the same considerations as for the field along the a axis. The polar and azimuthal angles of the γ-rays and the applied field were found to be 120(10)° and 45(20)° respectively. The fluctuation rates and the R_{tp} values as obtained from

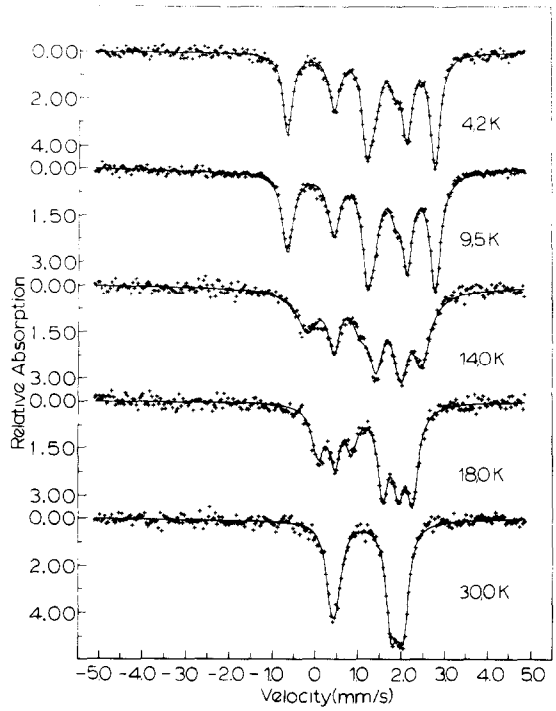

Fig. 12. Representative single crystal spectra of $RbFeCl_3 \cdot 2H_2O$ measured in a field of 1.5 T along the c axis. The solid lines represent the fit using the Blume and Tjon model.

these fits are plotted in figs. 13 and 11, respectively. The fluctuation rates follow the exponential behaviour over the whole frequency window of the MES. This is in accordance with suppression of the 3D ordering temperature by applying

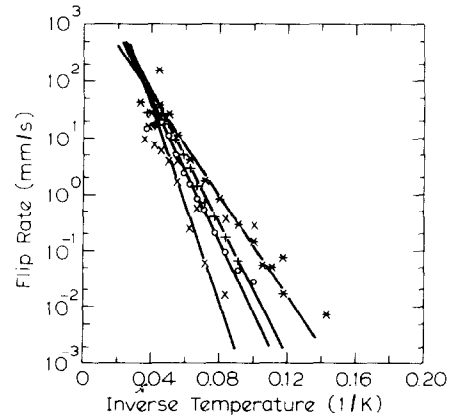

Fig. 13. The flip rate of the BT fits to the spectra of $RbFeCl_3 \cdot 2H_2O$ obtained with an applied field of 1.5 (*), 2.25 (+), 3.0 (○), and 6.0 (×) Tesla along the c-axis. The solid lines illustrate the activated processes.

magnetic fields larger than 1.24 T along the c axis. The activation energy appears to increase with increasing applied field. The solid lines in fig. 13 correspond to activation energies of 100(10), 130(15), 145(20), and 200(40) K. The R_{tp} values correspond quite well with the prediction for the Ising chain [30], where the canted spin configuration was represented by a ferromagnetic chain with $J_a/k_B = 39$ K and $B = (\mu_c/\mu_B)B_{app}$, where according to ref. [21] $\mu_c = 1.6\mu_B$.

4. Ideal kink gas

One of the commonly used non-linear differential equations in the theoretical literature on solitons is the sine–Gordon equation, which describes a continuous field ϕ as a function of position (in one dimension) and time [31],

$$\frac{d^2\phi}{dx^2} - \frac{1}{c_0^2}\frac{d^2\phi}{dt^2} = \frac{1}{2d^2}\sin(2\phi)\,. \tag{3}$$

This non-linear differential equation has as solutions solitons and breathers. Breathers are pulsory excitations that can be viewed as small amplitude kink–anti-kink pairs or inharmonic phonons [31]. We will not discuss the breathers, since they probably have a negligible effect on the presented results. The soliton solutions of eq. (3) can be written as

$$\phi(x,t) = 4\arctan\left[\exp\left(\pm\frac{\gamma}{d}(x - vt)\right)\right], \tag{4}$$

where d is the soliton width, $\gamma = (1 - (v/c_0)^2)^{-1/2}$, and c_0 is the soliton cut-off velocity. The solitons can be seen as relativistic pseudo-particles [31]. A characteristic feature of soliton solutions is that they are found in anisotropic systems and connect degenerate ground states. Solitons do not lose their initial velocity, and when colliding with each other or with impurities suffer only a phase shift [32]. The equation of motion for a system of coupled spins on a discrete chain can be mapped onto the sine–Gordon equation (eq. 3) under the following two assumptions: (i) the spins can be represented by classical vectors, and (ii) the continuum limit can be taken i.e. $\phi_i - \phi_{i+1} \to 0$ [33]. For the ferro- and antiferromagnetic chain systems, soliton solutions are illustrated in figs. 1a and 1b, respectively.

However, since both compounds investigated in this paper can best be described by the effective $S = \frac{1}{2}$ Hamiltonian,

$$\mathcal{H} = -2J\sum_i \left[S_i^z S_{i+1}^z + \tfrac{1}{2}\varepsilon(S_i^+ S_{i+1}^- + S_i^- S_{i+1}^+)\right], \tag{5}$$

where $S_i^{\pm} = S_i^x \pm iS_i^y$, the quantum mechanical treatment given by Maki [34] and Villain [35] will be followed. As long as $\varepsilon \ll 1$ and $J < 0$, the ground state of Hamiltonian (5) is well approximated by the Néel state. The excited states can be approximated by

$$|\cdots + - + - \vdots - + - + \cdots\rangle\,. \tag{6}$$

The spin configuration represented by (6) is illustrated in fig. 1c. Note that the overlap, ε, between two excited states, differing only in that the kink is shifted over two lattice sites, is non-zero, which guarantees the dynamic behaviour of the kinks. The theoretical prediction for the thermally averaged kink velocity is given by

$$v_k = \frac{4}{\pi}k_B T\left[I_0\left(\frac{2\varepsilon J}{k_B T}\right)\right]^{-1}\sinh\left(\frac{2\varepsilon J}{k_B T}\right), \tag{7}$$

where $I_0(z)$ is a modified Bessel function. The kink density is given by

$$n_k = \tfrac{1}{2}I_0\left(\frac{2\varepsilon J}{k_B T}\right)\exp\left(\frac{-|J|}{k_B T}\right). \tag{8}$$

The dynamics of a magnetic chain can be described by the spin correlation function. Only the parallel components are considered, for the reasons discussed above. In the free gas approximation for kinks, the spin–spin correlation function is given by [34]

$$\langle S^z(0,0)\,S^z(x,t)\rangle = \langle S^z\rangle^2\exp[i\pi x - 2N(x,t)]\,, \tag{9}$$

where $N(x, t) = n_k(x^2 + v_k^2 t^2)^{1/2}$. The quantity $\langle S^z \rangle^2$ for a pure Ising system equals S^2. It can be reduced by perpendicular spin components and by renormalization due to quantum and thermal effects [34], which in our Ising-type compounds can be neglected. As already stated, MES probes the autocorrelation function, which can easily be obtained by setting $x = 0$ in eq. (9), yielding

$$\langle S^z(0)\, S^z(t) \rangle = \langle S^z \rangle^2 \exp(-\Gamma_\omega t)\,, \qquad (10)$$

where $\Gamma_\omega = 2n_k v_k$ is the relaxation rate or flip rate.

Comparing the autocorrelation function as given in eq. (10) with the BT model [27, 28], one can infer that the ideal kink gas is based on precisely the same autocorrelation function as the BT model. Therefore, a comparison between the ideal kink gas and the experimental data is easily performed by analyzing the spectra using the BT model. As described in section 3, the following discrepancies result. Firstly, the MES line shape of the powder spectra does not fit the BT model (fig. 6). Secondly, the experimental activation energy is apparently a factor of two larger than the ideal soliton gas predicts. And finally, if we estimate $\varepsilon \approx 0.1$, the calculated flip rate for both compounds at 10 K exceeds the MES frequency window, which means that the ideal kink gas predicts a doublet over the complete temperature regime investigated. From these three major discrepancies one should conclude that the ideal kink gas is inadequate to describe the autocorrelation function as observed by the Mössbauer effect.

From the spin–spin correlation function (eq. 9), the static correlation function can easily be obtained:

$$\langle S^z(0)\, S^z(x) \rangle = \langle S^z \rangle^2 \exp(i\pi x - 2n_k x)\,. \qquad (11)$$

This indicates that if $\varepsilon = 0$, the 1D magnetic correlation length is equal to $\xi_{1D} = 1/(2n_k) = \exp(|J|/k_B T)$. This correlation length corresponds exactly to the prediction for the Ising chain. Quasi-elastic neutron diffraction and susceptibility (χ') measurements are experimental methods that are sensitive to the magnetic correlation length, and indeed, in such studies a correlation length in the chains is found that is proportional to the inverse kink density [3, 44]. This seems to be trivial. However, it has a strong implication for the interpretation of our experiments. Namely, a systematic observation of twice the kink energy implies that the autocorrelation function as probed by MES is *not* simply proportional to the kink density. Therefore, the basis of the ideal kink gas description, namely the fact that the relaxation rate is proportional to the product of kink density and velocity (eq. 9), breaks down.

Several deviations from the ideal kink gas have been dealt with in the theoretical literature. A number of papers have been devoted to the two approximations that are made to map a magnetic chain onto the sine–Gordon equation (3). The first approximation concerns the description of a discrete number of spins by a continuous field [29–31]. The second concerns the classical treatment of the spins. Dashen et al. [39] investigated the quantum mechanical analogue of the sine–Gordon equation, which gave comparable soliton-like excitations with renormalized soliton width and energy (to higher and lower values respectively). However, the description of Villain and Maki is based on the quantum mechanical chain Hamiltonian (eq. 5), such that the above two approximations, as well as their implications for the dynamics of the non-linear excitations, become irrelevant.

5. Phenomenological model

The excitation spectrum of the 1D Ising-type antiferromagnetic chain is known in the literature [40, 41]. It is illustrated in fig. 14a, which shows three possible classes of excitations. Two of them, the so-called inter-band excitations excite the chain from the ground state, namely the kink pair excitations (A) with energy $\sim 2|J|$, also referred to as magnon bound states [42], and the single kink excitations (B) with energy $\sim |J|$. The third class of excitations (C) contains intra-band excitations that couple two states in the continuum band around an energy of $2|J|$. The

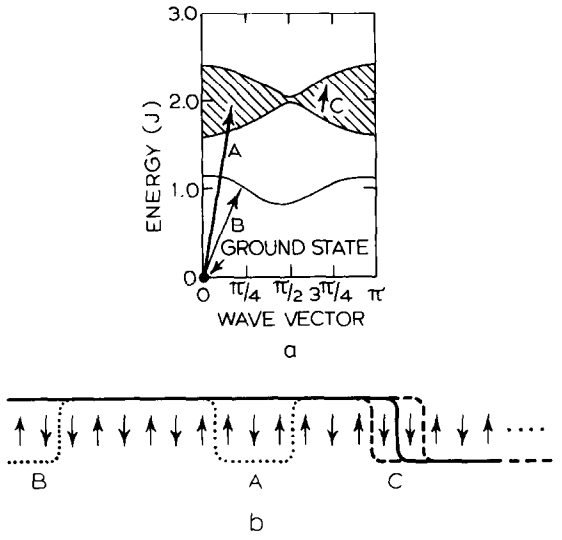

Fig. 14. (a) Excitation spectrum for a finite Ising-type antiferromagnetic chain system (taken from ref. [44]). (A) Kink pair or magnon bound state excitations, (B) single kink excitations created at the ends of the chain, and (C) intra-band excitations. (b) The same excitations are illustrated in an antiferromagnetic chain segment.

single kink excitations are only found in calculations of finite chains if free ends are considered instead of cyclic boundary conditions [26]. Moreover, for a chain with N spins, the statistical weight for exciting single kinks and kink pairs will be proportional to N and N^2 respectively. Therefore, experimentally, single kink excitations can safely be neglected for sufficiently long chains. Experimental methods like spin cluster excitation [43] and inelastic neutron scattering [44, 45] probe the excitation spectrum, and indeed find inter-band excitations with energies roughly equal to $2|J|$. In addition to these excitations, the latter experiments on $CsCoCl_3$ revealed also the presence of the intra-band excitations at much lower energies.

In MES experiments on powders, two distinct subspectra are observed up to temperatures above which the intensity of one of them becomes negligible. The first is the slowly relaxing subspectrum, which shows an activation energy of about $2|J|$. This subspectrum can be identified with the creation and annihilation of kink pairs. In fig. 14b, they are illustrated by the dotted line. This is in strong contrast to the ideal kink gas approximation, in which it is supposed that the kinks are present on basis of entropy considerations, and their displacement is responsible for the spin fluctuations. Since the kink pair excitations appear to be thermally activated, it is most probable that the coupling between the phonon bath and the spin system is responsible for their creation and annihilation. The present ferrous chain systems show strong spin–orbit coupling, which may provide for the thermal link between the phonon and the spin system [46]. A quantitative description of the proportionality constant that can be added to eq. (2) is at present not available in the literature, but a semi-quantitative approach to a related problem can be found in ref. [47]. The second subspectrum, the doublet, relaxes rapidly and shows a temperature independent relaxation rate. We identify this subspectrum with the intra-band excitations illustrated in fig. 14a. The level splittings in this kink pair band are small with respect to the temperature, resulting in a fast (paramagnetic) relaxation behaviour. We remark that these rapid fluctuations have to be restricted to limited regions of the chain during the characteristic Mössbauer time, since otherwise the slowly relaxing component would simply be not present. We will return to this point later. In a more phenomenological approach, one can consider the two spins which bracket the kink to be frustrated, since they experience two competing nearest neighbour interactions. Their two possible energy levels, corresponding to spin up and down, are degenerate (when neglecting the interchain interactions and the transverse interaction terms). An illustration can be found in fig. 14b. Since the flip rate is temperature independent, spin–spin interactions are thought to be responsible. If this assumption is true, the relaxation frequency of the order of 10^7 to 10^8 Hz corresponds to inter-spin distances of between the 10 and 15 Å, which is slightly larger than the interchain distance. The rapidly relaxing component in the spectra disappears if a magnetic field is applied (section 3.3). This is as expected, since an applied field polarizes the spins and lifts the degeneracy of their energy levels. The third type

of excitation in the Ising-type chain systems, the single kink excitation, is not observed for the reasons given above.

The relaxation behaviour observed at temperatures at which the intensity of the slowly relaxing subspectrum has become negligible is a result of the combination of the relaxation mechanisms that are depicted in fig. 14. The activation energy of the dominating relaxation mechanism will be observed. In RFC the dominating relaxation mechanism appears to be the thermal excitation of the kink pairs, since an activation energy of about $2|J|$ is found. Moreover, the measurements in an applied field, which suppresses the intra-band excitations, show the same activated process. In FOX, on the other hand, an activation energy of 70(10) K is found, which is comparable to $|J|/k_B$, indicating that the intraband excitations are dominant. Hence, the relaxation rate is proportional to the density of the kinks.

The phenomenological model presented here has already been applied in the work of ElMassalami [5, 6], who has performed AC susceptibility measurements between 10 and 10^5 Hz on the doped Ising-type ferromagnetic compounds $T_xFe_{1-x}Cl_2(Py)_2$ (where T is Ni, Cd, Mn, or Co, and Py is NC_5H_5). The real part, (χ'), as well as the imaginary part, (χ''), of the susceptibility as a function of frequency could be described by the superposition of two Debye curves. The susceptibility decreases from isothermal in the low frequency regime to adiabatic at high frequencies. The accompanying maxima in the χ'' showed activated processes, with activation energies of $|J|$ and $2|J|$, respectively. The AC field disturbs the equilibrium of the spin system. Thermal excitation of kinks at the ends of the chains and of kink pairs or magnon bound states reestablishes equilibrium. Enlarging the degree of doping evidently breaks up the magnetic chains and creates more ends. Indeed, in the χ'' experiment, the intensity of the relaxation of single kinks was enhanced in this way. Since the available frequency range was between 10 and 10^5 Hz, no indication of the intraband excitations was found in the susceptibility. However, complementary Mössbauer studies on these doped materials clearly demonstrate their presence [48].

6. Discussion

An important feature of the experimental results is the observation of two subspectra, each of which shows a separate relaxation mechanism.

The slowly relaxing subspectrum shows the thermal activation of kink pairs. This relaxation mechansim has not been considered in the ideal gas approximation. Moreover, for the interpretation of the neutron scattering experiments on TMMC and NMR measurements on TMMC and RFC, this kind of excitation is not taken into account. Since the characteristic measuring time for quasi-elastic neutron scattering, using thermal neutrons, is of the order of 10^{12} Hz, it is plausible that the creation of kink pairs does not influence the neutron data, although they are of dominant importance for interpreting the slowly relaxing Mössbauer subspectrum.

The second relaxation mechanism observed by the Mössbauer effect concerns the fast (paramagnetic) relaxation reflected in the doublet subspectrum. Since a part of the spectrum is relaxing much more slowly, the fast motion of the kinks should be restricted to finite regions of the chains only. The average length of the rapidly relaxing regions and the correlation length can be estimated to be 11 and 13 lattice units at 12.0 K for RFC and 74 and 124 lattice units at 15.0 K for FOX. Several mechanisms can be found in literature that may be able to explain the fact that one observes two subspectra. Firstly, repulsive forces between two kinks might be responsible. These are indeed found in the quantum sine–Gordon model in the strong coupling case for antiferromagnetic chains [49]. Secondly, one can think of impurities or lattice defects which have a pinning effect on the kinks. Thirdly, inter-chain interactions may restrict the motion of the kinks even above the 3D ordering temperature. In this respect, a comparison to thc random field problem, in which domain walls occur in monolayers of a noble gas on a substrate [50], or in a two-dimensional Ising system [51, 52], may be

made. Further study is needed, however, to explain the occurrence of the two subspectra. Furthermore, the fast relaxation mechanism might be related to a diffusive motion or random walk of the kinks. A necessary condition is then that this diffusive motion of the kinks is restricted to only parts of the chain during the characteristic MES time. In that case, a diffusive motion generates a rapidly relaxing subspectrum with a relative intensity that reflects the fraction of the spins that are subject to this motion. The diffusive kink model, as proposed in refs. [53, 54], describes the NMR data on both TMMC [9] and RFC [10] much better than the ideal kink gas. We want to return briefly to the results of the quasi-elastic neutron scattering on TMMC. During the characteristic time interval of quasi-elastic neutron scattering ($\sim 10^{-12}$ s), the ideal soliton gas predicts a displacement of the soliton of the order of one lattice unit (according to e.g. ref. [55], $v_s = 1.4 \times 10^{12}$ l.u./s). This might be the reason why the first experiments on TMMC could be interpreted in terms of an ideal soliton gas [55]. In later neutron scattering experiments, where a time resolution of the order of 10^9 to 10^{11} Hz was obtained in a spin-echo experiment, deviations from the ideal soliton description were found, and a diffusive propagation behaviour became of importance for the interpretation [11]. As regards the Mössbauer experiments, however, to the authors' knowledge no MES line shape has been calculated incorporating the autocorrelation function appropriate for kink diffusion or a random walk.

The relative intensity of the rapidly relaxing component increases with increasing temperature. Since the density of the kinks is proportional to $\exp(-|J|/k_B T)$, it is tempting to seek the same temperature dependence for the relative area of the doublet. This seems to be the case for FOX, see fig. 8, where an excitation energy of 73(10) K is found. The intensity of the doublet as a function of the inverse temperature for the RFC powder measurements is shown in fig. 9. Here the temperatures at which an activated process would be observable coincide with the 3D ordering. With the interpretation of the intensity of the rapidly relaxing component in terms of an activated process one should be careful, however, because the doublet intensity may also be influenced by the number of spins per kink that take part in the paramagnetic relaxation during the characteristic Mössbauer time. Moreover, the number of imperfections in the chain can change the kink density quite drastically, as is concluded in ref. [5, 6, 56].

The influence of 3D ordering in RFC is clearly reflected in the intensity of the rapidly relaxing subspectrum (fig. 9). We believe that, at this temperature, the total number of kinks decreases drastically, because of the onset of magnetic correlation in the directions perpendicular to that of the chain. At zero temperature, a perfect antiferromagnetic crystal would not include any kinks, in contrast to the ferromagnet, where demagnetization effects induce domains. Moreover, below the 3D ordering temperature, the relaxation rate no longer follows that of an activated process, irrespective of whether an applied field is present or not. This is also observed in e.g. $FeCl_2(Py)_2$ [3]. There is, however, no reason to assume that the coupling between the phonon and the spin system changes at the 3D ordering. This might indicate that the activated kink pairs, which propagate in the paramagnetic state, become frozen below the 3D ordering temperature. On the one hand, the propagation above T_N is in agreement with the overlap between the eigenstates of eq. (5), and on the other hand with the experimental results of NMR T_1^{-1} and neutron diffraction measurements. FOX does not give any indication of what happens at the 3D ordering temperature, since at this temperature the Mössbauer spectra are already fully split.

If an external field is applied upon RFC parallel to the ferromagnetic components of the spins, the activation energy of the kink pairs or magnon bound states appears to be strongly field dependent. Qualitatively this is evident, since the creation of kink pairs is accompanied by the loss of Zeeman energy of the spins located between these two kinks. It is evident that a quantitative interpretation of the loss of Zeeman energy is dependent on the angle the magnetic spins make with respect to the applied field,

which determines the size of the ferromagnetically aligned spin components. If one assumes that the angle of the spins with the applied field is field independent, a quantitative estimate of the average number of spins that are directed antiparallel to the field during the creation of a kink pair is of the order of ten. The fact that the direction of the internal hyperfine field is only slightly dependent on the applied field gives credence to this quantitative estimate. Moreover, the experimental data of the ratio of transition probabilities, R_{tp} as shown in fig. 11, are described quite nicely by a field independent ferromagnetic component.

7. Conclusion

In this paper we have studied the spin dynamics in the highly anisotropic quasi-1D magnetic systems $FeC_2O_4 \cdot 2H_2O$ and $RbFeCl_3 \cdot 2H_2O$, as probed by the Mössbauer effect. The first compound exhibits a large hyperfine field, which enhances the experimental resolution. This forced us to interpret the data at low temperatures in terms of two subspectra, with equal static MES parameters and with different relaxation rates, resulting from two relaxation mechanisms. The slowly relaxing subspectrum shows a thermal activated process with an activation energy $2|J|$. The fast relaxing component has a constant relaxation rate. The intensity of the latter component increases as a function of temperature. Above a certain temperature, only one spectrum can be distinguished. Upon applying a magnetic field, the fast relaxing subspectrum disappears. The activation energy increases with increasing field along the ferromagnetically aligned spin components.

The ideal gas description of non-interacting solitons is unable to describe the data because (i) the relaxation rate predicted by the ideal kink gas is far too high, (ii) the spectral line shape calculated with a single Markov process by the BT model does not fit the measured spectra, and (iii) the experimental activation energy is twice as large as predicted.

One can understand the observations by assuming (i) frustrated spin regions, where via spin–spin relaxation the flip rate is relatively high and temperature independent, and (ii) creation and annihilation of kink-pairs, involving energy exchange with the lattice.

Acknowledgements

We thank the group of Prof. Dr. W.J.M. de Jonge of the Technische Universiteit te Eindhoven for providing the $RbFeCl_3 \cdot 2H2O$ crystals. In the course of preparing the single crystal samples of $RbFeCl_3$ the assistance of Dr. R.H. Nussbaum of the Portland State University was indispensable. We are indebted to the group of Prof. Dr. F. Tuinstra of the Technische Universiteit te Delft for the use of their X-ray apparatus and acknowledge in particular A. van den Berg for his assistance. The present work is part of the research program of the "Stichting voor Fundamenteel Onderzoek der Materie" (Foundation for the Fundamental Research on Matter) and was made possible by financial support from the Nederlandse Organisatie voor Zuiver-Wetenschappelijk Onderzoek (Netherlands Organization for the Advancement of Pure Research).

References

[1] L.J. de Jongh, J. Appl. Phys. 53 (1982) 8018.
[2] R.C. Thiel, H. de Graaf and L.J. de Jongh, Phys. Rev. Lett. 47 (1981) 1415.
[3] H.J.M. de Groot, L.J. de Jongh, R.C. Thiel and J. Reedijk, Phys. Rev. B 30 (1984) 4041.
[4] H.J.M. de Groot, PhD. Thesis, Rijksuniversiteit te Leiden (1986).
[5] M. ElMassalami, H.H.A. Smit, H.J.M. de Groot, R.C. Thiel and L.J. de Jongh, in: Proc. in Phys. 23, Magnetic Excitations and Fluctuations II, eds. U. Balucani, S.W. Lovesey, M.G. Rasetti and V. Tognetti (Springer-Verlag, Berlin, 1987) p. 178.
[6] M. ElMassalami, PhD. Thesis, Rijksuniversiteit te Leiden (1987).
[7] H.H.A. Smit, H.J.M. de Groot, R.C. Thiel, L.J. de Jongh, C.E, Johnson and M.F. Thomas, Sol. State Commun. 53 (1985) 573.

[8] H. Th. Le Fever, PhD. Thesis, Rijksuniversiteit te Leiden (1980).
[9] J.P. Boucher, H. Benner, F. Devreux, L.P. Regnault, J. Rossat-Mignod, C. Dupas, J.P. Renard, J. Bouillot and W.G. Stirling, Phys. Rev. Lett. 48 (1982) 431.
[10] A.M.C. Tinus, C.J.M. Denissen, H. Nishihura and W.J.M. de Jonge, J. Phys. C 15 (1982) L791.
[11] J.P. Boucher, F. Mezei, L.P. Regnault and J.P. Renard, Phys. Rev. Lett. 55 (1985) 1778.
[12] J.P. Boucher, L.P. Regnault, R. Pynn, J. Bouillot and J.P. Renard, EuroPhys. Lett. 1 (1986) 415.
[13] P.C. Carić, Bull. Soc. Franç. Miner. Crist. LXXXXII (1959) 50.
[14] S. de S. Barros and S.A. Friedberg, Phys. Rev. 141 (1966) 637.
[15] F. de S. Barros, P. Zory and L.E. Campbell, Phys. Lett. 7 (1963) 135.
[16] P.C.M. Gubbens, A.M. van der Kraan, J.A.C. van Ooijen and J. Reedijk, J. de Phys. C2 (1979) 328.
[17] Jiing-Yann Chen, Satoru Simizu and S.A. Friedberg, J. Appl. Phys. 57 (1985) 3338.
[18] H.J.M. de Groot, L.J. de Jongh, M. ElMassalami, H.H.A. Smit and R.C. Thiel, Hyperf. Int. 27 (1986) 93.
[19] J.A.J. Basten, Q.A.G. van Vlimmeren and W.J.M. de Jonge, Phys. Rev. B 18 (1978) 2179.
[20] K. Kopinga, Q.A.G. van Vlimmeren, A.L.M. Bongaarts and W.J.M. de Jonge, Physica 86–88 B (1977) 671.
[21] Q.A.G. van Vlimmeren and W.J.M. de Jonge, Phys. Rev. B 19 (1979) 1503.
[22] M. Durieux, Metrologia 15 (1979) 65.
[23] H.H. Sample, B.L. Brandt and L.G. Rubin, Rev. Sci. Instrum. 53 (1982) 1129.
[24] H. Spiering, Hyp. Int. 3 (1977) 213.
[25] M.J. Clauser, Phys. Rev. B 3 (1971) 3748.
[26] J.D. Johnson and J.C. Bonner, Phys. Rev. B 22 (1980) 251.
[27] M. Blume and J.A. Tjon, Phys. Rev. 165 (1968) 446.
[28] M. Blume, Phys. Rev. 174 (1968) 351.
[29] F. Borsa, Phys. Lett. A80 (1980) 309.
[30] E. Ising, Z. Phys. 31 (1925) 253.
[31] A.R. Bishop, J.A. Krumhansl and S.E. Trullinger, Physica D 1 (1980) 1.
[32] M.B. Fogel, S.E. Trullinger, A.R. Bishop and J.A. Krumhansl, Phys. Rev. B 15 (1977) 1578.
[33] H.J. Mikeska, J. Phys. C 13 (1980) 2913; J. Appl. Phys. 52 (1981) 1950.
[34] K. Maki, in: Progress in Low Temperature Physics, Vol. VIII, ed. D.F. Brewer (North-Holland, Amsterdam, 1981).
[35] J. Villain, Physica B 79 (1975) 1.
[36] M. Peyrard and M.D. Krumhansl, Physica D 14 (1984) 88.
[37] C. Willis, M. El-Batanouny and P. Stancioff, Phys. Rev. B 33 (1986) 1904.
[38] J.F. Currie, S.E. Trullinger, A.R. Bishop and J.A. Krumhansl, Phys. Rev. B 15 (1977) 5567.
[39] R.F. Dashen, B. Hasslacher and N. Neveu, Phys. Rev. D 11 (1975) 3424.
[40] N. Ishimura and H. Shiba, Prog. Theor. Phys. 63 (1980) 743.
[41] H. Yoshizawa, K. Hirakawa, S.K. Satija and G. Shirane, Phys. Rev. B 23 (1981) 2298.
[42] J.B. Torrance Jr. and M. Tinkham, Phys. Rev. 187 (1969) 587, 595.
[43] Q.A.P. van Vlimmeren, C.H.W. Swüste, W.J.M. de Jonge, M.J.H. van der Steeg, J.H.M. Stoelinga and P. Wyder, Phys. Rev. B 21 (1980) 3005.
[44] S.E. Nagler, W.J.L. Buyers, R.L. Armstrong and B. Briat, Phys. Rev. B 2 (1983) 3873.
[45] W.J.L. Buyers, M.J. Hogan, R.L. Armstrong and B. Briat, Phys. Rev. B 33 (1986) 1727.
[46] R. Orbach, Proc. Roy. Soc. London, A 264 (1961) 458.
[47] M. Tinkham, Phys. Rev. 188 (1969) 967.
[48] M. ElMassalami and L.J. de Jongh, Paper II and M. ElMassalami, H.H.A. Smit, R.C. Thiel and L.J. de Jongh, Paper III, Physica B 154 (1989) 254, 267 (this issue).
[49] V.E. Korepin, Commun. Math. Phys. 76 (1980) 165.
[50] J. Villain, J. Phys. Lett. 43 (1982) L551.
[51] D.A. Huse and C.L. Henley, Phys. Rev. Lett. 54 (1985) 2708.
[52] T. Nattermann, J. Phys. C Phys. 18 (1985) 6661.
[53] K. Maki, Phys. Rev. B 24 (1981) 335.
[54] L. Gunther and Y. Imry, Phys. Rev. Lett. 44 (1980) 1225.
[55] J.P. Boucher and J.P. Renard, Phys. Rev. Lett. 45 (1980) 486.
[56] T. de Neef, J. Phys. Soc. Jpn. 37 (1974) 71.